 doi:10.20944/preprints202208.0048.v1

Article

Regulatory T Cell Depletion Using A CRISPR Fc-Optimized CD25 Antibody

Marit J. van Elsas[1], Johan M.S. van der Schoot[2], Alexander Bartels[2], Kas Steuten[2], Duco van Dalen[2,3], Zacharias Wijfjes[2,3], Carl G. Figdor[2], Thorbald van Hall[1], Sjoerd H. van der Burg[1], Martijn Verdoes[2,3,5]* and Ferenc A. Scheeren[4,5]*

[1] Department of Medical Oncology, Oncode Institute, Leiden University Medical Centre (LUMC), Albinusdreef 2, 2333ZA Leiden, The Netherlands
[2] Department of Tumor Immunology, Radboud Institute for Molecular Life Sciences, Radboud University Medical Centre, Geert Grooteplein 26, 6525GA Nijmegen, The Netherlands
[3] Institute for Chemical Immunology, Geert Grooteplein Zuid 28, 6525 GA, Nijmegen, Netherlands.
[4] Department of Dermatology, Leiden University Medical Centre (LUMC), Albinusdreef 2, 2333ZA Leiden, The Netherlands
[5] These authors contributed equally
* Correspondence: martijn.verdoes@radboudumc.nl, f.a.scheeren@lumc.nl;

Abstract: Regulatory T cells (T_{regs}) are major drivers behind immunosuppressive mechanisms and present a major hurdle for cancer therapy. T_{regs} are characterized by high expression of CD25, which is a potentially valuable target for T_{reg} depletion to alleviate immune suppression. The preclinical anti-CD25 (αCD25) antibody, clone PC-61, has met with modest anti-tumor activity, due to its capacity to clear T_{regs} from circulation and lymph nodes but not those that reside in the tumor. Optimization of the Fc domain of this antibody clone has been shown to enhance intratumoral T_{reg} depletion capacity. Here, we generated a stable cell line that produces optimized recombinant T_{reg} depleting antibodies. A genome engineering strategy in which CRISPR-Cas9 was combined with homology directed repair (CRISPR-HDR) was utilized to optimize the Fc domain of the hybridoma PC-61 for effector functions by switching it from the original rat IgG1 to a mouse IgG2a isotype. In a syngeneic tumor mouse model the resulting αCD25-m2a (mouse IgG2a isotype) antibody mediated effective depletion of tumor resident T_{regs} leading to a high effector T cell (T_{eff}) to T_{reg} ratio. Moreover, combination of the αCD25-m2a with αPD-L1 treatment augmented tumor eradication in mice, demonstrating the potential for αCD25 as a cancer immunotherapy.

Keywords: antibody; immunotherapy; CRISPR/HDR; FC optimization; hybridoma

1. Introduction

The presence of regulatory T-cells (T_{regs}) within the tumor contributes to a local environment in which effective anti-tumor immunity is actively dampened. In preclinical models, increasing numbers of T_{regs} support tumor manifestation, while their depletion leads to a delay in tumor growth [1–3]. In the clinic, a low ratio of effector T cells (T_{eff}) to T_{regs} (T_{eff}/T_{reg}) corresponds to poor reaction to immunotherapy while a high T_{eff}/T_{reg} ratio is associated with effective immunotherapy [4–6]. Targeted strategies to reduce the number of tumor infiltrating T_{regs} or to diminish their immunosuppressive effects can offer significant benefit in clinical cancer treatment. In particular the combination with T-cell stimulatory immunotherapies such as the use of checkpoint inhibitors or generation of tumor specific T cell responses via vaccination regimens with tumor-specific antigens may improve therapy [7–9].

The recent clinical success of antibody-based immune checkpoint inhibitors in various malignancies has led to a surge in the development of novel immune modulators that alleviate immune suppression in the tumor microenvironment (TME) [10,11]. The thera-

 doi:10.20944/preprints202208.0048.v1

peutic efficacy of these antibodies was first thought to be solely mediated by Fab' mediated blockade of inhibitory signaling from T_{regs}. However, recent preclinical and clinical evidence suggest that Fc mediated mechanism are a major determinant in leveraging therapy in checkpoint targeted treatments [12–14]. Use of Fc optimized αCTLA4 results in superior tumor control in mouse models and the presence of high affinity fragment crystallizable (Fc) receptor (FcR) polymorphism in patients treated with αCTLA4 ipilimumab correlates with increased survival for these patients [14,15]. Therefore, the use of depletion inducing backbones in antibodies targeting surface proteins highly expressed on T_{regs} could be a valuable strategy to potentiate the efficacy of existing therapeutic antibodies and leverage cancer immunotherapy.

CD25, also known as the interleukin-2 high-affinity receptor alpha chain (IL-2Rα), represents a valuable target for antibody-mediated depletion of T_{regs}. This receptor is highly expressed on T_{regs} and, in combination with CD4 and forkhead boxP3 (FoxP3) expression, used for identification of this immune suppressive cell type [16]. CD25 has been used as a target for development of antibody-based therapeutics in past studies, and although preclinical and clinical studies demonstrated that these antibodies can actively deplete T_{regs}, their anti-tumor activity *in vivo* remained modest [3,17–19]. The clone PC-61 is a widely used anti-murine CD25 antibody that depletes T_{regs} *in vitro*, but is rather ineffective at depleting T_{regs} within established tumors [2,20]. This is attributed to the isotype of PC-61, being rat IgG1, that exhibits a low preference for activating over inhibiting Fc gamma receptors, which is a strong determinant for its therapeutic potential [21,22]. Others demonstrated that exchanging the immune inert rat IgG1 Fc domain for the classical depleting mouse IgG2a Fc domain results in augmented anti-tumor activity of PC-61 [23]. This αCD25-m2a version effectively depleted intratumor T_{regs} in mouse models, increased intratumoral T_{eff}/T_{reg} ratios, and in combination with αPD-1 treatment effectively eradicated tumors *in vivo* [23].

We are interested in αCD25-m2a as a sole T_{reg} depleting agent, which would allow us to study the underlying dynamics and timing of T_{reg} depletion and subsequent T_{eff} generation. We recently demonstrated efficient engineering of the immunoglobulin heavy chain locus of hybridomas by combining CRISPR-Cas9 (Clustered regular interspaced short palindromic repeats - CRISPR associated protein 9) with homology directed repair (HDR) [24]. This allows the rapid generation of stable cell lines that secrete isotype variants of the parental antibody without losing specificity for the original target. Here, we used this platform to obtain recombinant αCD25-m2a and evaluated its efficacy in combination with programmed death ligand 1 (PD-L1) treatment for cancer immunotherapy.

2. Results

CRISPR-HDR can be used to optimize the PC-61 hybridoma

To engineer the immunoglobulin locus of the rat IgG1 PC-61 hybridoma (Figure 1A) we utilized a guide RNA (gRNA) which directs the Cas9 nuclease to a protospacer adjacent motif (PAM) located in an intron upstream of the exon encoding the CH1 domain of rat IgG1 (Figure S1). Additionally, we designed an HDR donor construct to resolve the Cas9 mediated double stranded break and insert an synthetic exon consisting of an artificial splice acceptor, the murine IgG2a Fc domain, a sortag and his-tag and gene elements to convert blasticidin resistance (Figure 1B, Table S1). After co-transfection of PC-61 hybridomas we applied selection pressure with blasticidin to enrich for hybridoma clones which successfully integrated the donor construct. After one week, we confirmed secretion of proteins with the his-tag in the supernatant of the selected hybridoma population and performed limiting dilution to obtain monoclonal cell lines. His-tag positive monoclonal supernatants as determined by dot-blot (Figure 1C) were exposed to $CD25^+$ target cells in combination with secondary antibodies against murine IgG2a or rat IgG1 to select

Preprints (www.preprints.org) | NOT PEER-REVIEWED | Posted: 2 August 2022 doi:10.20944/preprints202208.0048.v1

for a recombinant hybridoma that exclusively expressed CD25 binding antibodies of the murine IgG2a isotype (Figure 1D). Reliable quantification of the insertion is not possible, as only hybridomas with successful insertion will survive. However, this approach has a success rate of 100%, meaning that every genomic engineering experiment using a single specific HDR donor construct resulted in multiple correctly engineered hybridoma clones after selection (Figure 1C,D). Based on the exclusive and high expression of murine IgG2a, we selected the recombinant hybridoma clone PC-61_B2 for production of αCD25-m2a. After cultivation of PC-61_B2, we isolated αCD25-m2a from the supernatant using his-tag affinity purification. We subsequently cleaved off the his-tag via sortase (srt) mediated hydrolysis [25] (Figure 1E,F) to circumvent the potential his-tag associated liver retention of antibodies [26]. Notably, within a fraction of the αCD25-m2a the use of sortase-mediated cleavage of the his-tag resulted in intramolecular covalent linkage of the heavy chains (Figure S2), likely through nucleophilic addition of the ε-amino group of the lysine present near the c-terminus to the sortase activated c-terminus of the adjacent heavy chain [27].

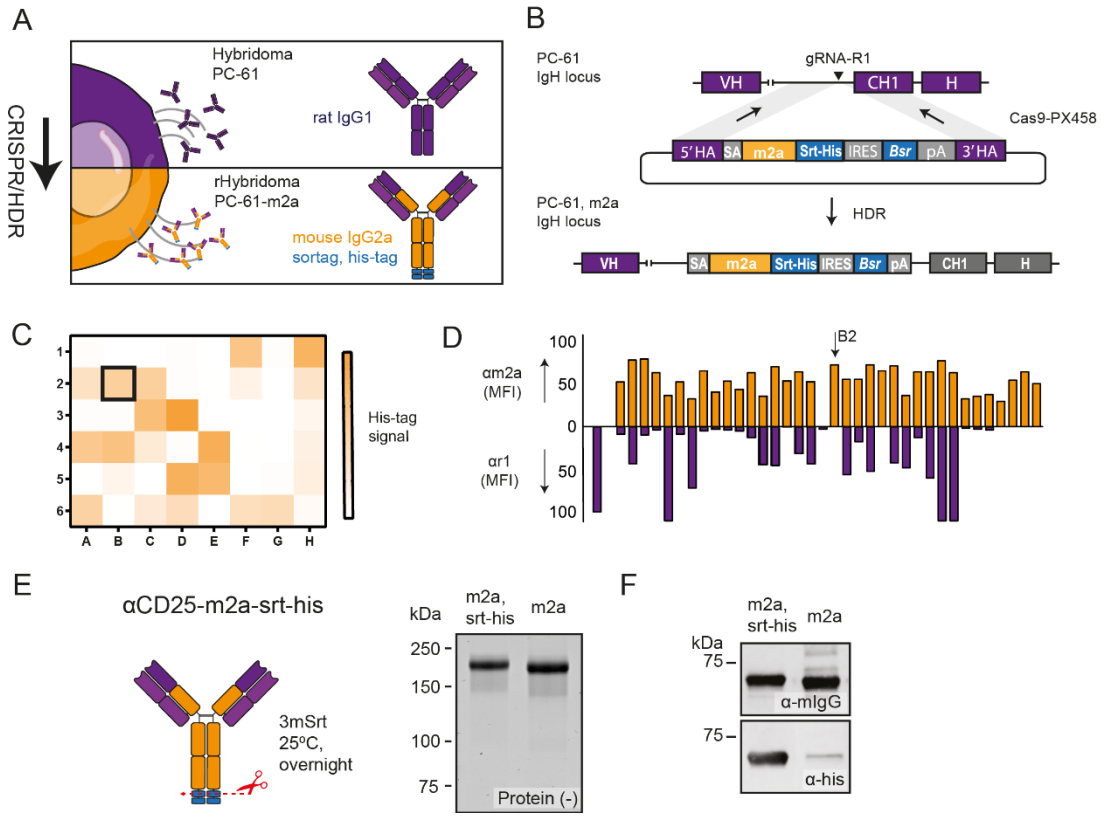

Figure 1. **CRISPR-HDR mediated FC optimization of PC-61 hybridoma. (A) Schematic of CRISPR/HDR engineering to tune expression of PC-61 hybridoma from rat IgG1 to mouse IgG2a. (B) The IgH locus of PC-61 is targeted with gRNA-R1 to create a double stranded break that can be repaired through homology with the donor construct that will insert the murine IgG2a Fc domain with c-terminal sortag and his-tag (srt-his) and gene elements for blasticidin resistance. (C) Supernatant HDR and gRNA-R1 transfected cells that were resistant to blasticidin were taken and screened for secretion of his-tag positive antibodies via dotblot. (D) His-tag positive supernatants were used to stain activated splenocytes in combination with secondary antibodies against mouse IgG2a (yellow) and rat IgG1 (violet) to select engineered hybridoma that exclusively secreted m2a antibodies targeting CD25. The selected PC-61-m2a clone for antibody**

 doi:10.20944/preprints202208.0048.v1

production is indicated (B2). (E) His-tag removal of PC-61-m2a via sortase mediated hydrolysis with non-reducing SDS-page and immunoblot (F). *αCD25-m2a efficiently depletes T_{regs} resulting in an increased T_{eff}/T_{reg} ratio*

To evaluate the T_{reg} depletion efficiency of our αCD25-m2a we tested the antibody in the syngeneic MC38 colon adenocarcinoma *in vivo* tumor model (Figure 2A). As the activity of the original antibody αCD25-r1 has been well studied by others, we opted to not use αCD25-r1, but only an isotype control (IgG2a) reference group for ethical reasons. We administered 200μg of αCD25-m2a on day 5 and 7 after inoculating mice with MC38 and evaluated T-cell populations within the blood, draining lymph node and tumor on day 9. Treatment with αCD25-m2a reduced the fraction of CD25 expressing cells in the $CD4^+$ T cell compartment (Figure 2B,C), decreased the percentage of $CD4^+FoxP3^+$ T_{regs} (Figure 2C) and increased the T_{eff}/T_{reg} ratios (Figure 2C) in the blood, draining lymph nodes and tumor. Depletion of $CD25^+FoxP3^+$ $CD4^+$ T cells was near complete in all compartments (Figure S3). Importantly, the depletion of effector $CD4^+$ and $CD8^+$ T cells was less dramatic compared to the depletion of T_{regs} (Figure S3). Only the percentage of intratumoral $CD8^+$ T_{effs} ($CD8^+CD25^+$) and $CD4^+$ T_{eff} in the tumor and draining lymph nodes ($CD25^+FoxP3^-$), but not that of the circulating T_{effs}, was significantly decreased (Figure S3).

Preprints (www.preprints.org) | NOT PEER-REVIEWED | Posted: 2 August 2022 doi:10.20944/preprints202208.0048.v1

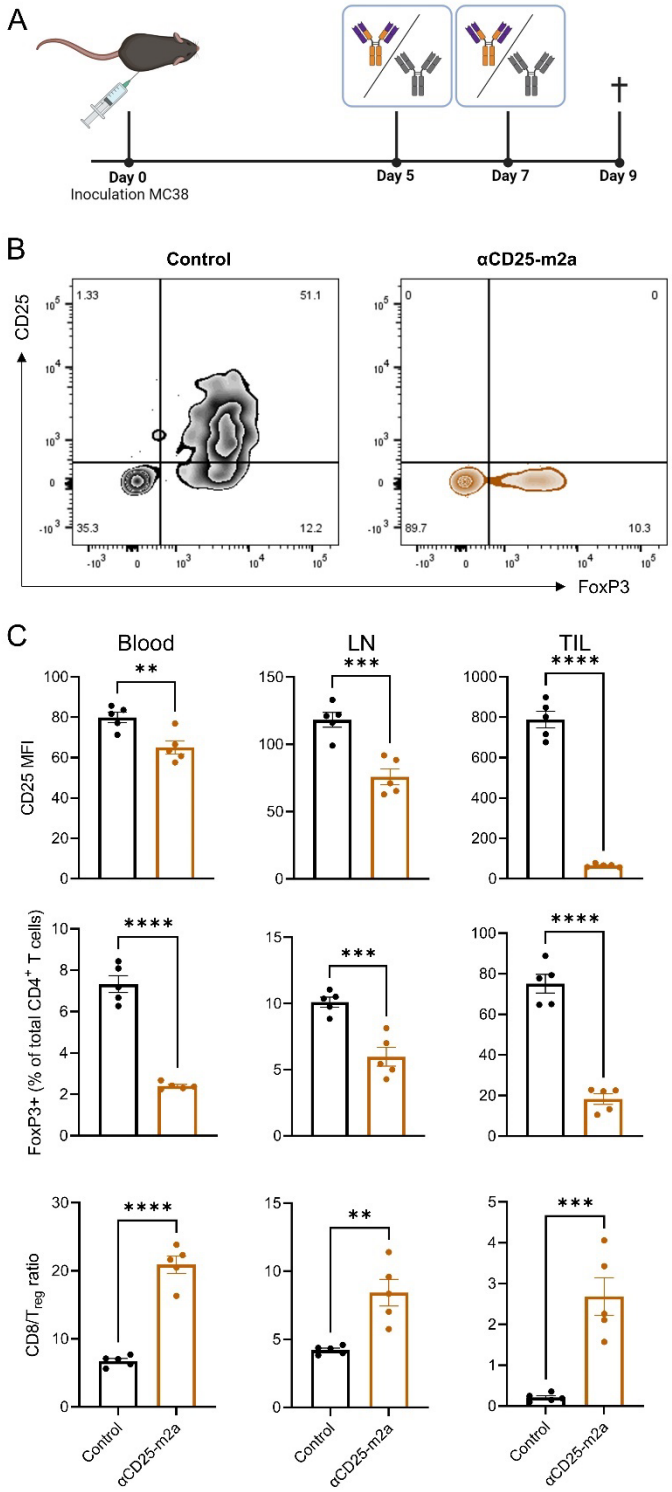

Figure 2. Effective depletion of T_{regs} in blood, lymph nodes and tumor via Fc-optimized αCD25-m2a. (A) Schematic of tumor challenge in C57/Bl6 mice. On day 0 mice were inoculated subcutaneously with MC38 and on day 5 and 7 treated with either αCD25-m2a or an isotype control. Blood, lymph nodes and tumor were harvested on day 9. (B) Representative plots showing expression of CD25 and FoxP3 in $CD3^+CD4^+$ T cells isolated from tumor. Numbers show percentage of cells in each quadrant. (C) MFI of CD25 in T_{regs}, percentage of T_{reg} cells in $CD3^+CD4^+$ T cells, and T_{eff}/T_{reg} cell ratios in blood, lymph nodes and tumor are shown (n=5, statistical difference determined via independent student t-test: *p≤0.05, ** p≤0.01, *** p≤0.001).

 doi:10.20944/preprints202208.0048.v1

CD25-m2a treatment synergizes with αPD-L1 treatment.

Having established that αCD25-m2a efficiently depletes tumor infiltrating T_{regs}, we wanted to explore its therapeutic efficacy in controlling tumor growth. Moreover, as antibodies targeting the PD-1/PD-L1 axis increase T_{eff} function and anti-tumor activity, we hypothesized that αCD25 would synergize with αPD-L1 in combinational therapy. Therefore, we inoculated mice with MC38 and injected 200µg αCD25-m2a at day 5 and day 7, injected 200µg the αPD-L1 clone 10F.9G2 (rat IgG2b) at day 5, day 8 and day 11, or combined the two treatment regimens and measured tumor growth over 60 days (Figure 3A). Although monotherapy with αCD25-m2a or αPD-L1 treatment resulted in the respective survival of 2/10 and 2/9 mice at the endpoint of the study, tumor growth in most mice was not delayed and comparable to the control group (Figure 3B,C). Of note, mice that responded to αCD25-m2a treatment experienced tumor regression as late as 30 days after tumor inoculation, indicating CD25 mediated depletion of T_{regs} has a delayed impact on tumor growth. By combining αCD25-m2a and αPD-L1 treatment the number of mice responding to therapy was increased (8/9) resulting in significant improvement in survival and response rates (6/9) at study termination compared to other treatments ($p<0.05$, Figure 3C, D). Also here a delayed response was observed similar to the responders in the αCD25-m2a monotherapy group. Taken together, these data demonstrate that the recombinant αCD25-m2a antibody stably produced by our CRISPR/HDR engineered PC-61 hybridoma is able to efficiently deplete T_{regs} from the TME and synergizes with αPD-L1 treatment of MC38 mouse colon adenocarcinoma.

Preprints (www.preprints.org) | NOT PEER-REVIEWED | Posted: 2 August 2022 doi:10.20944/preprints202208.0048.v1

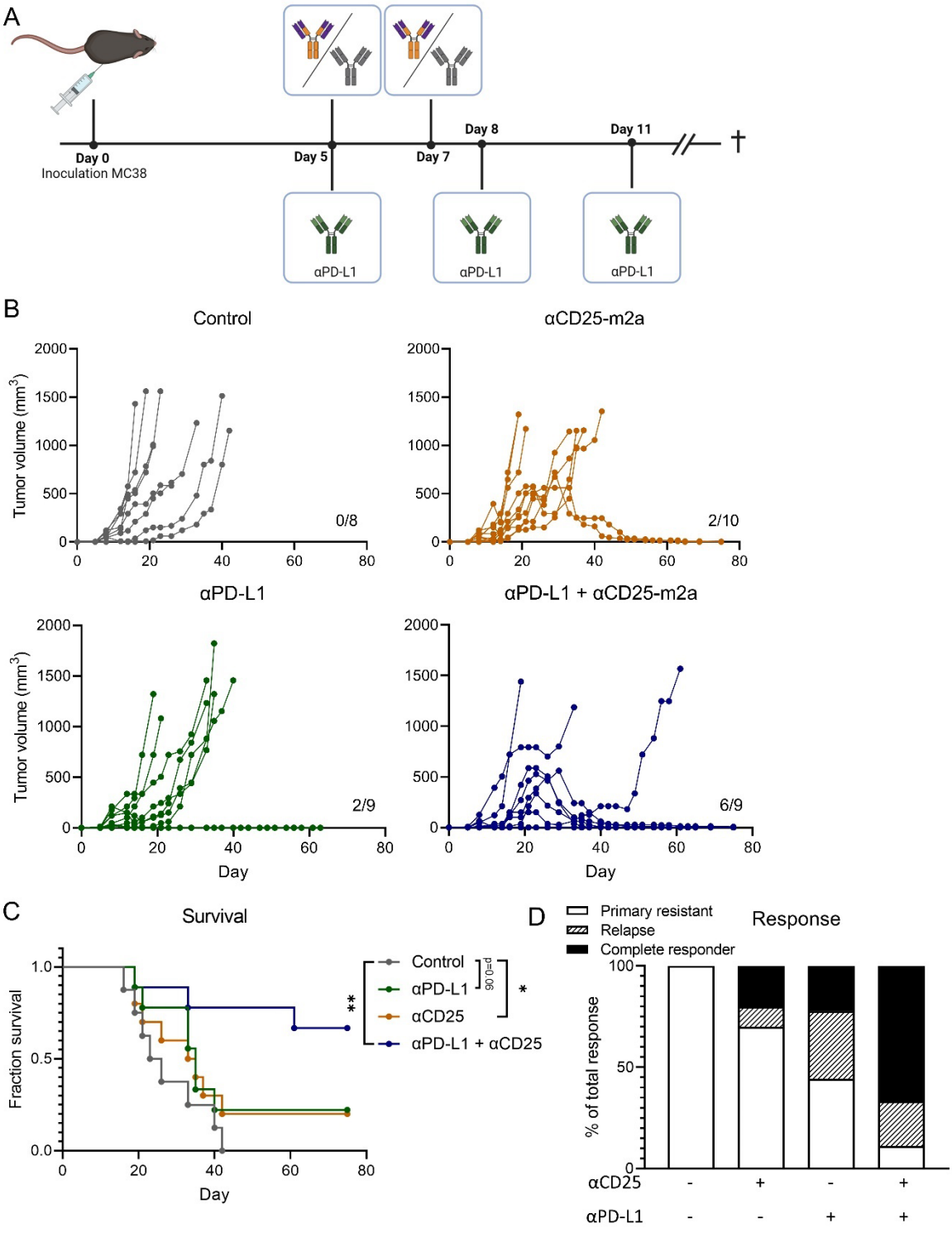

Figure 3. CD25-m2a treatment synergizes with αPD-L1 treatment. (A) Schematic of treatment schedule of C57/BL6 mice inoculated with MC38. On day 0 mice were inoculated subcutaneously with MC38 and subsequently treated on day 5 and 7 with αCD25-m2a or an isotype control, or treated on day 5, 8 and 11 with αPD-L1, or received both αCD25-m2a and αPD-L1 treatment. Mice were euthanized when tumors reached a volume of 1500mm³. (B) Growth curves of MC38 tumors. Number of tumor-free survivors is shown in each graph. (C) Survival curves and (D) response rates of mice shown in (B) (n=8-10, statistical difference determined via log rank test). Significance is shown as * = p<0.05, ** = p<0.01, and *** = p<0.001.

 doi:10.20944/preprints202208.0048.v1

Continued T_{reg} depletion does not affect therapeutic efficacy

The expression of CD25 is not limited to T_{regs} but is also present on activated $CD4^+$ and $CD8^+$ T cells. Indeed, treatment with CD25-m2a resulted in a decrease in intratumoral activated $CD4^+$ and $CD8^+$ T_{eff} cells (Figure S3). Despite this decrease, the observed durable tumor control led us to hypothesize that this activated $CD4^+$ and $CD8^+$ T_{eff} cell population is more rapidly renewed, compared to the T_{reg} population, resulting in a beneficial T_{eff}/T_{reg} ratio. To test this hypothesis, we treated MC38 tumor bearing mice with 200µg αCD25-m2a at day 5 and day 7 (short-term), or with 200µg αCD25-m2a at day 5, 7, 11, 16, 20 and 25 (continued), in combination with 200µg αPD-L1 (Figure 4A). Surprisingly, continued T_{reg} depletion did not affect the tumor control, as 4/8 mice had a durable tumor control, compared to 6/10 in the short-term depletion group ($p=0.63$, Figure 4B-D). This suggests a low replenishment rate of T_{regs} in the tumor, as no benefit on tumor control or survival could be observed. Moreover, as also no negative effect on survival was seen following continued αCD25-m2a treatment, we conclude that continued αCD25-m2a treatment does not negatively affect the anti-tumor immune response.

Preprints (www.preprints.org) | NOT PEER-REVIEWED | Posted: 2 August 2022 doi:10.20944/preprints202208.0048.v1

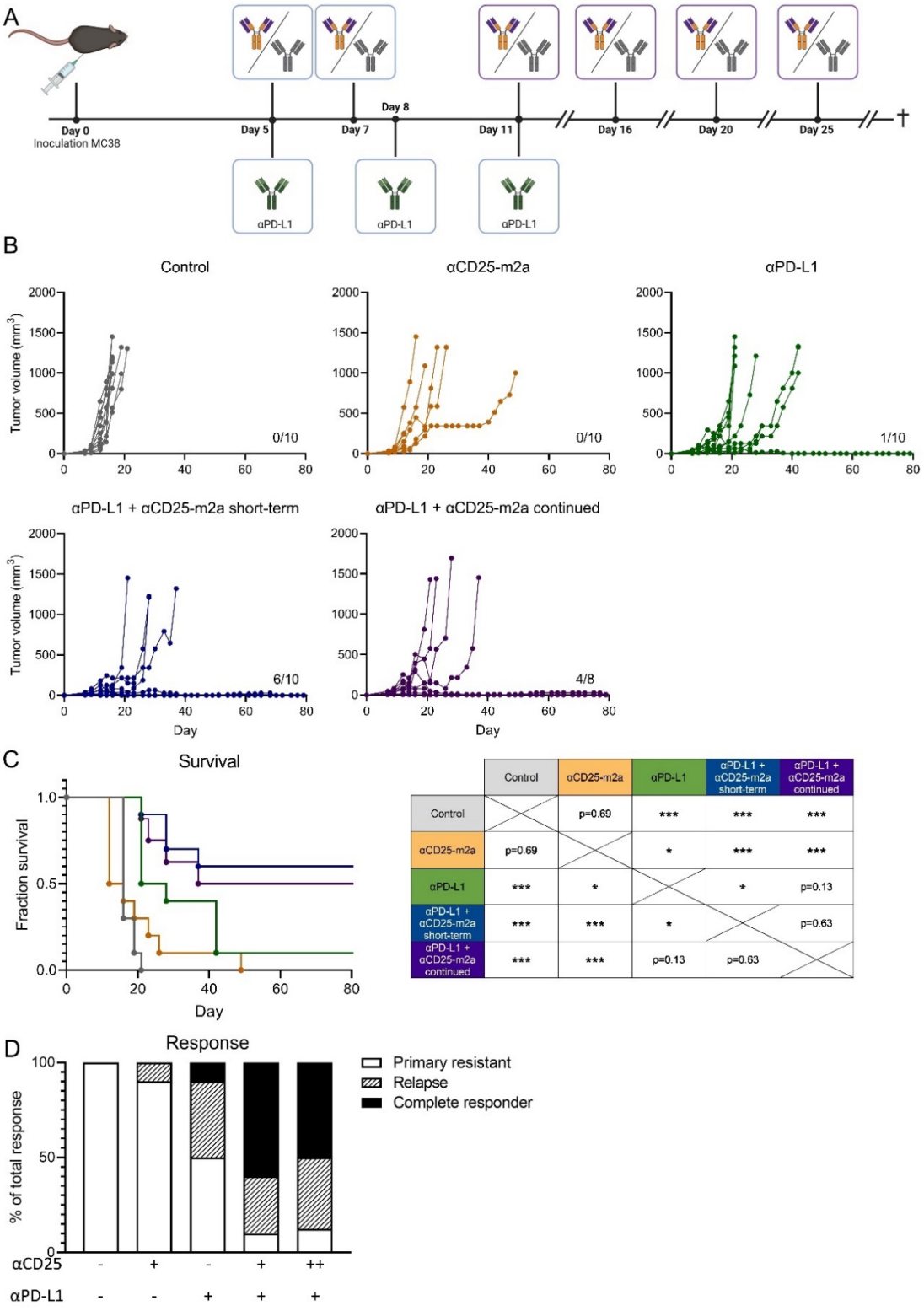

Figure 4. Continued T_{reg} depletion does not affect therapeutic efficacy. (A) Schematic of treatment schedule of C57/BL6 mice inoculated with MC38. On day 0 mice were inoculated subcutaneously with MC38 and subsequently treated on day 5 and 7 with αCD25-m2a (short-term) or day 5, 7, 11, 16, 20 and 25 (continued) or an isotype control, or treated on day 5, 8 and 11 with αPD-L1, or received both αCD25-m2a and αPD-L1 treatment. Mice were euthanized when tumors reached a volume of 1500mm³. (B) Growth curves of MC38 tumors. Number of tumor-free survivors is shown in each graph. (C) Survival curves including significance table and (D) response rates of mice shown in (B) (n=8-10, statistical difference determined via log rank test). Significance is shown as * = p<0.05, ** = p<0.01, and *** = p<0.001.

 doi:10.20944/preprints202208.0048.v1

3. Discussion

Here we described the generation of a stable cell line continuously producing recombinant Fc optimized anti-murine CD25 antibody PC-61 with enhanced immunotherapeutic activity for cancer treatment. For this purpose we performed CRISPR/HDR engineering of the parental hybridoma and exchanged its immune inert rat IgG1 Fc domain for the classical depleting murine IgG2a backbone (Figure 1A). Genetic engineering was effective, as we were able to identify multiple cell lines that secreted CD25 specific antibodies of murine IgG2a isotype with the designed chemoenzymatic- and his-tag. After isolation and his-tag removal, we performed tumor challenging studies with αCD25-m2a and demonstrated that the Fc optimized antibody can efficiently deplete T_{regs} from the TME (Figure 2). This is in contrast to the original PC-61 clone with rat IgG1 isotype that is unable to clear tumor infiltrating T_{regs} and demonstrated modest anti-tumor activity *in vivo* in combination with other therapies [28,29]. Moreover, αCD25-m2a treatment synergized with αPD-L1 treatment, leading to effective elimination of tumors and a significant increase in survival compared to using either treatment alone (Figure 3) [2,20]. Together, these results demonstrate that CRISPR/HDR can be used to repurpose hybridomas and their antibodies for cancer immunotherapy.

Besides increasing therapy efficacy, reduction of treatment associated toxicities has become a priority for the development of novel immunotherapeutic treatments. In the clinic, ipilimumab is one of the most commonly used immunotherapies and therapeutic efficacy has been attributed not only to the blocking of CTLA-4 function, but also to the depletion of T_{regs} [30]. However, ipilimumab is also associated with the development of severe immune-related toxicities, which may be attributed to activation of T_{eff} recognizing self-antigens [31–34]. In comparison to αCTLA-4 treatment, we hypothesize that αCD25 treatment can offer a larger therapeutic window as CD25 lacks the immune modulatory capacity compared to CTLA-4. Therefore, our results warrant further investigation of αCD25 as a potential therapeutic.

In this study we show αCD25-m2a treatment synergized with αPD-L1 treatment, resulting in superior tumor control and increased survival *in vivo* (Figure 3). Whereas αCD25-m2a treatment alleviates the tumor suppression by T_{reg} depletion, αPD-L1 treatment is known to block PD-L1 ligation to PD-1 on activated T cells, which circumvents impairment of T cell function [35,36]. Therefore, the PD-L1 blockade promotes the activity of the T_{eff} compartment within the TME. However, this particular αPD-L1 clone, 10F.9G2, has multiple mechanisms of action and can, besides blockade of the PD-1/PD-L1 axis, directly deplete tumor cells as well as certain myeloid populations within the tumor [37]. Therefore, extrapolation of which mechanism contributes to the synergistic effect is difficult and will be explored in future work by characterization of T cell and myeloid populations at different time points during and after treatment.

In the past, CD25 received a lot of attention as a potential target for cancer immunotherapy as it is used for the identification and isolation of T_{regs}. This lack of T_{reg} depleting efficacy in the tumor of the PC-61 antibody can be attributed to the rat IgG1 isotype and differential FcγR expression of effector cells in circulation, blood and tumor. Specifically, FcγR engagement of rat IgG1 is limited to the inhibiting FcγRIIb and activating FcγRIII and can therefore only recruit effector cells for T_{reg} depletion when these express low levels of FcγRIIb [38]. In circulation and lymph nodes macrophages express low levels of FcγRIIb and can therefore be recruited for T_{reg} depletion [23]. In contrast, macrophages in the TME express high levels of FcγRIIb, impairing macrophage activation and depletion of T_{regs} [23,39]. The use of the mIgG2a isotype backbone in PC-61, which interacts besides FcγRIIb and FcγRIII with the activating FcγRI and FcγRIV [40], can overcome this inhibitory signaling of FcγRIIb and may license tumor-associated macrophages for T_{reg} deple-

 doi:10.20944/preprints202208.0048.v1

tion. These observations underline the importance of evaluating different antibody formats early-on in development to select an optimal design that augments its therapeutic potential as demonstrated by others [41,42].

Depletion of T_{regs} by CD25-targeting antibodies has already been tested in a clinical trial in combination with a dendritic cell (DC) cancer vaccine [43]. Despite a successful clearance of T_{regs} from the circulation of these patients, no effect on progression-free survival could be observed, compared to the DC vaccine single treatment. This lack of response has been attributed to the αCD25-mediated depletion of activated $CD25^+$ effector T cells, required for a DC vaccine-induced tumor control. In line with these findings, we also found that despite the favorable T_{eff}/T_{reg} ratio in the tumor, the number of activated T_{effs} are decreased as well, as determined by the percentage of $CD25^+$ cells in the $CD8^+$ T cell compartment on day 9 (Figure S3). The reduction of activated T_{effs} within the tumor offers an explanation for the delayed response to αCD25-m2a / αPD-L1 treatment. Surprisingly, even after continued depletion of $CD25^+$ T cells by CD25-m2a, a durable tumor control was observed (Figure 4). Therefore, we have established that this subset of activated $CD25^+CD8^+$ T cells, that is depleted by CD25-m2a, is not crucial for the anti-tumor T cell activity. Elegant efforts to circumvent this undesirable depletion of $CD25^+$ T_{eff} cells by αCD25 targeting antibodies have been undertaken, resulting in the development of a non-IL-2 blocking αCD25 antibody [44]. By resolving the variable region of the anti-CD25 clone 7D4 and cloning it into a mouse IgG2a backbone, they managed to generate a T_{reg} depleting antibody while preserving the T_{eff} function. Future research will determine whether the use of such an antibody could also improve therapeutic efficacy in the clinic.

To negate possible detrimental *in vivo* effects of the c-terminal his-tag on Fc-optimized αCD25-m2a antibodies we performed the sortase-mediated hydrolysis of the heavy chain. Although the his-tag was successfully removed, we observed an additional protein band of approximately 120kDa in size as determined by reducing SDS-page (Figure S2). Given that mass spectrometry measurements and non-reducing SDS-page confirm the final products to be monomeric and of the expected size, we postulate that sortase-mediated reaction leads to covalent inter-heavy chain linkage within a single antibody molecule. Likely, the acyl-enzyme intermediate that is formed during the reaction is not resolved via hydrolysis, but via a nucleophilic attack from the ε-amino side chain of a lysine of the opposing heavy chain in close proximity to the c-terminus, linking the chains together [27]. Although the formation of these bonds did not influence antibody performance, it could be prevented by providing an excess of nucleophilic peptides during sortase-mediated reaction, or by simply removing the protein tags from the original HDR design.

Here, we adapted our previously developed CRISPR/HDR engineering approach [24] to modify several rat IgG2a hybridomas and obtain antibodies in the format and isotype of choice to accommodate engineering of the rat IgG1 locus. The efficient generation of daughter cell lines secreting αCD25-m2a antibodies underline the versatility of this approach as it can be adapted and applied to virtually any hybridoma. Such an approach can be advantageous over conventional transient techniques as i) no knowledge regarding Ig DNA sequences hybridomas is needed but only the isotype needs to be determined, ii) a stable continuous source of antibody product is preferred over transient systems, and iii) the expertise and funds to use of transient expression systems is not available.

Preprints (www.preprints.org) | NOT PEER-REVIEWED | Posted: 2 August 2022 doi:10.20944/preprints202208.0048.v1

4. Materials and Methods

CRISPR-HDR engineering. The genomic sequence of the IgH locus of rat IgG1 was identified via the Ensembl rate genome build Rnor_6.0 for gRNA and donor construct design. The donor construct was ordered as a synthetic gene from IDT and cloned into a vector via traditional cloning techniques. The gRNAs, including gRNA-R1 (CATCCTCCATTTATACAGCC), used for this study were designed with the CRISPR tool from the Zhang laboratory and cloned into the pX330-U6-Chimeric_BB-CBh-hSpCas9 vector, which was obtained as a kind gift from F. Zhang (Addgene ref:42230) [45]. PC-61 hybridomas were transfected with donor construct and gRNA-R1 and cultivated for 10 days under blasticidin pressure. The resulting blasticidin resistant population diluted in 96-well plates to 0.3 cells/well to obtain monoclonal cell lines. Plates were cultured until wells could be observed with high cell concentrations. From each monoclonal cell line, 3 µL supernatant was spotted on a nitrocellulose membrane and allowed to dry at RT for one hour. Subsequently, the nitrocellulose membrane was stained with rabbit antibody against his-tag (ab137839, Abcam) and goat antibody against rabbit (926-32211, LI-COR) to select for resistant modified hybridomas that expressed his-tagged antibodies. His-tag positive supernatants were used to stain CD3 and CD28 stimulated splenocytes from Bl6 mice and subsequently screened with anti-mIgG2a-PE (12-4210-82, ThermoFisher) and anti-rIgG1-APC (17-4812-82) to identify daughter cell lines that exclusively secrete murine IgG2a that bind CD25. Detailed description of CRISPR-HDR editing of hybridomas can be found elsewhere [24].

Antibody production and isolation. For αPC-61-m2a, 20 million PC-61_B2 cells were seeded in CELLine Bioreactor Flasks (900-05, Argos) and cultivated for 1 week. Antibody-containing supernatants were separated from cells via centrifugation (90g, 5 min), filtered through a 20-µm filter, and supplemented with 10 mM imidazole (I2399, Sigma-Aldrich). Subsequently, the hybridoma supernatant was run over an Ni-NTA column (30210, Qiagen) and washed with 10 column volumes of PBS supplemented with 10 mM imidazole before antibody elution with PBS supplemented with 250 mM imidazole. Buffer exchange to PBS was performed via ultracentrifugation with Amicon Ultra-15 centrifugal filter units (Z717185, Sigma-Aldrich). WT antibodies from PC-61 were obtained by cultivating parental hybridoma using CD Hybridoma medium (11279023, Thermo Fisher Scientific) supplemented with 2 mM ultraglutamine, 1× AA, and 50 µM 2-ME. PC-61 were purified from medium using Protein G GraviTrap (28-9852-55, Sigma-Aldrich) according to the manufacturer's protocol. Antibody concentration was determined via absorption at 280 nm with an extinction coefficient of 1.4 using a Nanodrop 2000 (Thermo Fisher Scientific). Protein purity was assessed by reducing SDS-PAGE using the SYPRO Ruby Protein Gel Stain (S12000, Thermo Fisher Scientific).

Sortase mediated hydrolysis. For his-tag removal, αCD25-m2a was dialyzed into sortase buffer (150 mM tris, 50 mM NaCl, and 10 mM $CaCl_2$, pH 7.5) via ultracentrifugation. Sortase-mediated reaction was carried out with 15 mg of αCD25-m2a with 0.5 equivalents of trimutant sortase A Δ59 (3M srt) [46] in a volume of 1.5 mL overnight at RT. Subsequently the reaction volume was increased to 5 mL and adjusted to a concentration of 10 mM imidazole before it was incubated with 2 mL Ni NTA resin to remove 3M srt, unreacted αCD25-m2a, and cleaved his-tag. The column was washed twice with PBS supplemented with 10 mM imidazole, after which the flow through containing the hydrolyzed product was collected and dialyzed against PBS. Concentration was determined via absorption at 280 nm with an extinction coefficient of 1.4 using a Nanodrop 2000 (Thermo Fisher Scientific) and analyzed on reducing and non-reducing SDS-page to assess purity. His-tag removal of the αCD25-m2a was assessed by Western blot stained with anti-Histag rabbit antibody (ab213204, Abcam) visualized by anti-rabbit IRDye800 (926-32211, LI-COR) and anti-mouse IRDye600 (9260-32220, LI-COR).

Tumor experiments. For assessing T_{reg} depletion, female C57/BL6 mice were injected subcutaneously in their right flank with $5x10^5$ MC38 cells resuspended in 200µL PBS supplemented with 0,1% BSA. To two cohorts of five mice 200µg of αCD25-m2a or an isotype

 doi:10.20944/preprints202208.0048.v1

control (IgG2a, InVivoPlus BioXCell) were administered intraperitoneally on day 5 and 7. Tumor volume was measured on day 5, 7 and 9, after which the mice were euthanized. Blood, lymph nodes and tumors were harvested and processed for phenotyping using flow cytometry. Used anti-mouse antibodies for flow cytometry were anti-CD4-BV711 (563050, BD Bioscience), anti-CD25-FITC (553072, BD Bioscience), anti-CD8-PerCP-Cy5.5 (551162, BD Bioscience), anti-FoxP3-PE (560046, BD Bioscience), anti-CD3-APC (100235, Biolegend) and anti-CD45-aF700 (103127, Biolegend). For tumor challenge, nine cohorts of ten female C57/BL6 mice each, were injected subcutaneously in their right and left flank with $5x10^5$ MC38 cells resuspended in 200µL PBS supplemented with 0,1% BSA on day 0. All *in vivo* experiments were performed with 8-10 animals per group and performed once. For the control and short-term αCD25-m2a cohort, mice received the same treatment as described above. For the continued αCD25-m2a cohort, additional treatments with 200µg of αCD25-m2a were administered at day 11, 16, 20 and 25. For all the αPD-L1 treatment cohorts, mice were injected on day 7 with an isotype control in 100µL PBS and injected on day 5, 8 and 11 with 200 µg of αPD-L1 (BE0101, BioXcell). Tumor volume was determined every other day and mice were euthanized when the tumor volume reached $1500mm^3$. Mice were maintained under specific pathogen–free conditions. All mouse experiments were controlled by the animal welfare committee (IvD) of the Leiden University Medical Center and approved by the national central committee of animal experiments (CCD) under the permit number AVD1160020197864, in accordance with the Dutch Act on Animal Experimentation and EU Directive 2010/63/EU.

Data Analysis. Flow cytometry data were analyzed with FlowJo v10 (Tree Star). Statistical analyses were done with Prism 8 (GraphPad Software); p values were calculated using independent student T tests (ns $p > 0.05$; *$p \leq 0.05$; **$p \leq 0.01$; ***$p \leq 0.001$). Kaplan-Meier curves were analyzed with the log-rank Mantel-Cox test.

Supplementary Materials: Figure S1: Genomic sequence of rat IgG1 heavy chain locus, Figure S2: Sortase mediated his-tag removal leads to covalent inter heavy chain linkage in αCD25-m2a, Figure S3: $CD25^+$ T-cell subsets in blood, lymphnodes and tumor from mice treated with αCD25-m2a or an isotype control, Table S1: HDR donor construct

Author Contributions: Conceptualization, F.A.S., M.Ve., C.G.F., and T.v.H..; methodology, M.J.v.E., J.M.S.S., C.G.F., T.v.H., S.H.B. F.A.S., and M.Ve.; validation M.J.v.E, J.M.S.S, A.B, K.S., D.D., and Z.W.; formal analysis, F.A.S, M.Ve., T.v.H., S.H.v.d.B.; performed experiments, M.J.v.E, J.M.S.S, A.B, K.S., D.D., and Z.W.; data curation, M.J.v.E. and J.M.S.S.; writing—original draft preparation, M.J.v.E, J.M.S.S M.Ve., and F.A.S; writing—review and editing, M.J.v.E, J.M.S.S., M.Ve., and F.A.S;; visualization, M.J.v.E. and J.M.S.S.; supervision, T.v.H., S.H.v.d.B., M.V., and F.A.S.; funding acquisition, M.Ve., S.H.v.d.B., and F.A.S. All authors have read and agreed to the published version of the manuscript.

Funding: M.V. is the recipient of ERC Starting grant CHEMCHECK (679921) and a Gravity Program Institute for Chemical Immunology tenure track grant by NWO. F.A.S. is the recipient of an LUMC Strategic fund (#049−19). M.J.v.E. was funded by the Oncode Base Fund to Senior Investigator S.H.v.d.B.

Data Availability Statement: The data needed to evaluate the conclusions are present in the paper and/or the Supplementary Materials. The described plasmids used in this study are deposited in plasmid repository of Addgene (www.addgene.org/). Additional data and materials related to this paper may be requested from the authors.

Acknowledgments: We thank S. van Duijnhoven (Radboudumc, Nijmegen, The Netherlands) for providing the 3 M sortase A and Camilla Labrie for technical assistance. We would also like to thank the animal and flow core facilities of the LUMC, Leiden, The Netherlands.

Conflicts of Interest: The authors declare no conflict of interest.

References

1. Elpek, K.G.; Lacelle, C.; Singh, N.P.; Yolcu, E.S.; Shirwan, H. CD4+CD25+ T Regulatory Cells Dominate Multiple Immune Evasion Mechanisms in Early but Not Late Phases of Tumor Development in a B Cell Lymphoma Model. *J. Immunol.* **2007**, *178*, 6840–6848, doi:10.4049/JIMMUNOL.178.11.6840.
2. Emma Jones; Michaela Dahm-Vicker; Anna Katharina Simon; Angharad Green; Fiona Powrie; Vincenzo Cerundolo; Awen Gallimore Depletion of CD25+ Regulatory Cells Results in Suppression of Melanoma Growth and Induction of Autoreactivity in Mice - PubMed. *Cancer Immun.* **2002**, *2*.
3. Denise Golgher; Emma Jones; Fiona Powrie; Tim Elliot; Awen Gallimore Depletion of CD25+ Regulatory Cells Uncovers Immune Responses to Shared Murine Tumor Rejection Antigens - PubMed. *Eur. J. Immunol.* **2002**, *32*, 3267–3275.
4. Shang, B.; Liu, Y.; Jiang, S.J.; Liu, Y. Prognostic Value of Tumor-Infiltrating FoxP3+ Regulatory T Cells in Cancers: A Systematic Review and Meta-Analysis. *Sci. Reports 2015 51* **2015**, *5*, 1–9, doi:10.1038/srep15179.
5. Hodi, F.S.; Butler, M.; Oble, D.A.; Seiden, M. V.; Haluska, F.G.; Kruse, A.; MacRae, S.; Nelson, M.; Canning, C.; Lowy, I.; et al. Immunologic and Clinical Effects of Antibody Blockade of Cytotoxic T Lymphocyte-Associated Antigen 4 in Previously Vaccinated Cancer Patients. *Proc. Natl. Acad. Sci. U. S. A.* **2008**, *105*, 3005–3010, doi:10.1073/PNAS.0712237105/SUPPL_FILE/12237FIG6.JPG.
6. Quezada, S.A.; Peggs, K.S.; Curran, M.A.; Allison, J.P. CTLA4 Blockade and GM-CSF Combination Immunotherapy Alters the Intratumor Balance of Effector and Regulatory T Cells. *J. Clin. Invest.* **2006**, *116*, 1935–1945, doi:10.1172/JCI27745.
7. Goding, S.R.; Wilson, K.A.; Xie, Y.; Harris, K.M.; Baxi, A.; Akpinarli, A.; Fulton, A.; Tamada, K.; Strome, S.E.; Antony, P.A. Restoring Immune Function of Tumor-Specific CD4+ T Cells during Recurrence of Melanoma. *J. Immunol.* **2013**, *190*, 4899–4909, doi:10.4049/JIMMUNOL.1300271.
8. Bos, P.D.; Plitas, G.; Rudra, D.; Lee, S.Y.; Rudensky, A.Y. Transient Regulatory T Cell Ablation Deters Oncogene-Driven Breast Cancer and Enhances Radiotherapy. *J. Exp. Med.* **2013**, *210*, 2435, doi:10.1084/JEM.20130762.
9. Quezada, S.A.; Peggs, K.S.; Simpson, T.R.; Shen, Y.; Littman, D.R.; Allison, J.P. Limited Tumor Infiltration by Activated T Effector Cells Restricts the Therapeutic Activity of Regulatory T Cell Depletion against Established Melanoma. *J. Exp. Med.* **2008**, *205*, 2125, doi:10.1084/JEM.20080099.
10. Postow, M.A.; Callahan, M.K.; Wolchok, J.D. Immune Checkpoint Blockade in Cancer Therapy. *J. Clin. Oncol.* **2015**, *33*, 1974–1982, doi:10.1200/JCO.2014.59.4358.
11. Kyi, C.; Postow, M.A. Checkpoint Blocking Antibodies in Cancer Immunotherapy. *FEBS Lett.* **2014**, *588*, 368–376, doi:10.1016/J.FEBSLET.2013.10.015.
12. Heier, I.; Hofgaard, P.O.; Brandtzæg, P.; Jahnsen, F.L.; Karlsson, M. Depletion of CD4+ CD25+ Regulatory T Cells Inhibits Local Tumour Growth in a Mouse Model of B Cell Lymphoma. *Clin. Exp. Immunol.* **2008**, *152*, 381–387, doi:10.1111/J.1365-2249.2008.03642.X.
13. Bulliard, Y.; Jolicoeur, R.; Windman, M.; Rue, S.M.; Ettenberg, S.; Knee, D.A.; Wilson, N.S.; Dranoff, G.; Brogdon, J.L. Activating Fc γ Receptors Contribute to the Antitumor Activities of Immunoregulatory Receptor-Targeting Antibodies. *J. Exp. Med.* **2013**, *210*, 1685–1693, doi:10.1084/JEM.20130573.
14. Selby, M.J.; Engelhardt, J.J.; Quigley, M.; Henning, K.A.; Chen, T.; Srinivasan, M.; Korman, A.J. Anti-CTLA-4 Antibodies of IgG2a Isotype Enhance Antitumor Activity through Reduction of Intratumoral Regulatory T Cells. *Cancer Immunol. Res.* **2013**, *1*, 32–42, doi:10.1158/2326-6066.CIR-13-0013/471049/P/ANTI-CTLA-4-ANTIBODIES-OF-IGG2A-ISOTYPE-ENHANCE.

15. Vargas, F.A.; Furness, A.J.S.; Litchfield, K.; Joshi, K.; Rosenthal, R.; Ghorani, E.; Solomon, I.; Lesko, M.H.; Ruef, N.; Roddie, C.; et al. Fc Effector Function Contributes to the Activity of Human Anti-CTLA-4 Antibodies. *Cancer Cell* **2018**, *33*, 649, doi:10.1016/J.CCELL.2018.02.010.
16. S. Sakaguchi; N. Sakaguchi; M. Asano; M. Itoh; M. Toda Immunologic Self-Tolerance Maintained by Activated T Cells Expressing IL-2 Receptor Alpha-Chains (CD25). Breakdown of a Single Mechanism of Self-Tolerance Causes Various Autoimmune Diseases. | The Journal of Immunology. *J. Immunol.* **1995**, *155*, 1151–1164.
17. Setiady, Y.Y.; Coccia, J.A.; Park, P.U. In Vivo Depletion of CD4+FOXP3+ Treg Cells by the PC61 Anti-CD25 Monoclonal Antibody Is Mediated by FcgammaRIII+ Phagocytes. *Eur. J. Immunol.* **2010**, *40*, 780–786, doi:10.1002/EJI.200939613.
18. Rech, A.J.; Mick, R.; Martin, S.; Recio, A.; Aqui, N.A.; Powell, D.J.; Colligon, T.A.; Trosko, J.A.; Leinbach, L.I.; Pletcher, C.H.; et al. CD25 Blockade Depletes and Selectively Reprograms Regulatory T Cells in Concert with Immunotherapy in Cancer Patients. *Sci. Transl. Med.* **2012**, *4*, 134ra62, doi:10.1126/SCITRANSLMED.3003330.
19. Jacobs, J.F.M.; Punt, C.J.A.; Lesterhuis, W.J.; Sutmuller, R.P.M.; Brouwer, H.M.L.H.; Scharenborg, N.M.; Klasen, I.S.; Hilbrands, L.B.; Figdor, C.G.; De Vries, I.J.M.; et al. Dendritic Cell Vaccination in Combination with Anti-CD25 Monoclonal Antibody Treatment: A Phase I/II Study in Metastatic Melanoma Patients. *Clin. Cancer Res.* **2010**, *16*, 5067–5078, doi:10.1158/1078-0432.CCR-10-1757/83601/AM/DENDRITIC-CELL-VACCINATION-IN-COMBINATION-WITH.
20. Jun Shimizu; Sayuri Yamazaki; Shimon Sakaguchi Induction of Tumor Immunity by Removing CD25+CD4+ T Cells: A Common Basis Between Tumor Immunity and Autoimmunity | The Journal of Immunology. *J. Immunol.* **1999**, *163*, 5211–5218.
21. Dilillo, D.J.; Ravetch Correspondence, J. V Differential Fc-Receptor Engagement Drives an Anti-Tumor Vaccinal Effect ADCC-Mediated Tumor Clearance Requires Engagement of HFcgRIIIA on Macrophages d Selective Engagement of HFcgRIIA on DCs Promotes Long-Term Immunity against Cancer. *Cell* **2015**, *161*, 1035–1045, doi:10.1016/j.cell.2015.04.016.
22. Nimmerjahn, F.; Ravetch, J. V. Fcγ Receptors as Regulators of Immune Responses. *Nat. Rev. Immunol. 2007 81* **2008**, *8*, 34–47, doi:10.1038/nri2206.
23. Arce Vargas, F.; Furness, A.J.S.; Solomon, I.; Joshi, K.; Mekkaoui, L.; Lesko, M.H.; Miranda Rota, E.; Dahan, R.; Georgiou, A.; Sledzinska, A.; et al. Fc-Optimized Anti-CD25 Depletes Tumor-Infiltrating Regulatory T Cells and Synergizes with PD-1 Blockade to Eradicate Established Tumors. *Immunity* **2017**, *46*, 577, doi:10.1016/J.IMMUNI.2017.03.013.
24. Van Der Schoot, J.M.S.; Fennemann, F.L.; Valente, M.; Dolen, Y.; Hagemans, I.M.; Becker, A.M.D.; Le Gall, C.M.; Van Dalen, D.; Cevirgel, A.; Van Bruggen, J.A.C.; et al. Functional Diversification of Hybridoma-Produced Antibodies by CRISPR/HDR Genomic Engineering. *Sci. Adv.* **2019**, *5*, doi:10.1126/SCIADV.AAW1822/SUPPL_FILE/AAW1822_SM.PDF.
25. Mao, H.; Hart, S.A.; Schink, A.; Pollok, B.A. Sortase-Mediated Protein Ligation: A New Method for Protein Engineering. *J. Am. Chem. Soc.* **2004**, *126*, 2670–2671, doi:10.1021/JA039915E/SUPPL_FILE/JA039915ESI20040106_035555.PDF.
26. Hagemans, I.M.; Wierstra, P.J.; Steuten, K.; Molkenboer-Kuenen, J.D.M.; van Dalen, D.; ter Beest, M.; van der Schoot, J.M.S.; Ilina, O.; Gotthardt, M.; Figdor, C.G.; et al. Multiscale Imaging of Therapeutic Anti-PD-L1 Antibody Localization Using Molecularly Defined Imaging Agents. *J. Nanobiotechnology* **2022**, *20*, 1–15, doi:10.1186/S12951-022-01272-5/FIGURES/6.
27. Möhlmann, S.; Mahlert, C.; Greven, S.; Scholz, P.; Harrenga, A. In Vitro Sortagging of an Antibody Fab

Fragment: Overcoming Unproductive Reactions of Sortase with Water and Lysine Side Chains. *ChemBioChem* **2011**, *12*, 1774–1780, doi:10.1002/CBIC.201100002.

28. Matsushita, N.; Pilon-Thomas, S.A.; Martin, L.M.; Riker, A.I. Comparative Methodologies of Regulatory T Cell Depletion in a Murine Melanoma Model. *J. Immunol. Methods* **2008**, *333*, 167, doi:10.1016/J.JIM.2008.01.012.
29. Wu, L.; Yun, Z.; Tagawa, T.; Rey-McIntyre, K.; Anraku, M.; De Perrot, M. Tumor Cell Repopulation between Cycles of Chemotherapy Is Inhibited by Regulatory T-Cell Depletion in a Murine Mesothelioma Model. *J. Thorac. Oncol.* **2011**, *6*, 1578–1586, doi:10.1097/JTO.0B013E3182208EE0.
30. Wolchok, J.D.; Kluger, H.; Callahan, M.K.; Postow, M.A.; Rizvi, N.A.; Lesokhin, A.M.; Segal, N.H.; Ariyan, C.E.; Gordon, R.-A.; Reed, K.; et al. Nivolumab plus Ipilimumab in Advanced Melanoma. *N. Engl. J. Med.* **2013**, *369*, 122–133, doi:10.1056/NEJMOA1302369/SUPPL_FILE/NEJMOA1302369_DISCLOSURES.PDF.
31. Brahmer, J.R.; Lacchetti, C.; Schneider, B.J.; Atkins, M.B.; Brassil, K.J.; Caterino, J.M.; Chau, I.; Ernstoff, M.S.; Gardner, J.M.; Ginex, P.; et al. Management of Immune-Related Adverse Events in Patients Treated with Immune Checkpoint Inhibitor Therapy: American Society of Clinical Oncology Clinical Practice Guideline. *J. Clin. Oncol.* **2018**, *36*, 1714–1768, doi:10.1200/JCO.2017.77.6385.
32. Walunas, T.L.; Lenschow, D.J.; Bakker, C.Y.; Linsley, P.S.; Freeman, G.J.; Green, J.M.; Thompson, C.B.; Bluestone, J.A. CTLA-4 Can Function as a Negative Regulator of T Cell Activation. *Immunity* **1994**, *1*, 405–413, doi:10.1016/1074-7613(94)90071-X.
33. Ise, W.; Kohyama, M.; Nutsch, K.M.; Lee, H.M.; Suri, A.; Unanue, E.R.; Murphy, T.L.; Murphy, K.M. CTLA-4 Suppresses the Pathogenicity of Self Antigen–Specific T Cells by Cell-Intrinsic and Cell-Extrinsic Mechanisms. *Nat. Immunol. 2009 112* **2009**, *11*, 129–135, doi:10.1038/ni.1835.
34. Paterson, A.M.; Sharpe, A.H. Taming Tissue-Specific T Cells: CTLA-4 Reins in Self-Reactive T Cells. *Nat. Immunol. 2010 112* **2010**, *11*, 109–111, doi:10.1038/ni0210-109.
35. Sunshine, J.; Taube, J.M. PD-1/PD-L1 Inhibitors. *Curr. Opin. Pharmacol.* **2015**, *23*, 32–38, doi:10.1016/J.COPH.2015.05.011.
36. Iwai, Y.; Ishida, M.; Tanaka, Y.; Okazaki, T.; Honjo, T.; Minato, N. Involvement of PD-L1 on Tumor Cells in the Escape from Host Immune System and Tumor Immunotherapy by PD-L1 Blockade. *Proc. Natl. Acad. Sci. U. S. A.* **2002**, *99*, 12293–12297, doi:10.1073/PNAS.192461099/ASSET/0E18DCD1-4D55-4829-AD15-01D16A1FBDD7/ASSETS/GRAPHIC/PQ1924610004.JPEG.
37. Dahan, R.; Sega, E.; Engelhardt, J.; Selby, M.; Korman, A.J.; Ravetch, J. V. FcγRs Modulate the Anti-Tumor Activity of Antibodies Targeting the PD-1/PD-L1 Axis. *Cancer Cell* **2015**, *28*, 285–295, doi:10.1016/J.CCELL.2015.08.004.
38. Clynes, R.A.; Towers, T.L.; Presta, L.G.; Ravetch, J. V. Inhibitory Fc Receptors Modulate in Vivo Cytoxicity against Tumor Targets. *Nat. Med. 2000 64* **2000**, *6*, 443–446, doi:10.1038/74704.
39. Dahan, R.; Barnhart, B.C.; Li, F.; Yamniuk, A.P.; Korman, A.J.; Ravetch, J. V. Therapeutic Activity of Agonistic, Human Anti-CD40 Monoclonal Antibodies Requires Selective FcγR Engagement. *Cancer Cell* **2016**, *29*, 820–831, doi:10.1016/J.CCELL.2016.05.001.
40. J€, F.; Bruhns, P.; Onsson, F.J.; Roopenian, D. Mouse and Human FcR Effector Functions. *Immunol. Rev.* **2015**, *268*, 25–51, doi:10.1111/IMR.12350.
41. Chiu, M.L.; Goulet, D.R.; Teplyakov, A.; Gilliland, G.L. Antibody Structure and Function: The Basis for Engineering Therapeutics. *Antibodies (Basel, Switzerland)* **2019**, *8*, 55, doi:10.3390/ANTIB8040055.
42. Oostindie, S.C.; Lazar, G.A.; Schuurman, J.; Parren, P.W.H.I. Avidity in Antibody Effector Functions and Biotherapeutic Drug Design. *Nat. Rev. Drug Discov. 2022* **2022**, 1–21, doi:10.1038/s41573-022-00501-8.

43. Jacobs, J.F.M.; Punt, C.J.A.; Lesterhuis, W.J.; Sutmuller, R.P.M.; Brouwer, H.M.L.H.; Scharenborg, N.M.; Klasen, I.S.; Hilbrands, L.B.; Figdor, C.G.; De Vries, I.J.M.; et al. Dendritic Cell Vaccination in Combination with Anti-CD25 Monoclonal Antibody Treatment: A Phase I/II Study in Metastatic Melanoma Patients. *Clin. Cancer Res.* **2010**, *16*, 5067–5078, doi:10.1158/1078-0432.CCR-10-1757/83601/AM/DENDRITIC-CELL-VACCINATION-IN-COMBINATION-WITH.
44. Solomon, I.; Amann, M.; Goubier, A.; Arce Vargas, F.; Zervas, D.; Qing, C.; Henry, J.Y.; Ghorani, E.; Akarca, A.U.; Marafioti, T.; et al. CD25-Treg-Depleting Antibodies Preserving IL-2 Signaling on Effector T Cells Enhance Effector Activation and Antitumor Immunity. *Nat. Cancer 2020 112* **2020**, *1*, 1153–1166, doi:10.1038/s43018-020-00133-0.
45. Cong, L.; Ran, F.A.; Cox, D.; Lin, S.; Barretto, R.; Habib, N.; Hsu, P.D.; Wu, X.; Jiang, W.; Marraffini, L.A.; et al. Multiplex Genome Engineering Using CRISPR/Cas Systems. *Science (80-.).* **2013**, *339*, 819–823, doi:10.1126/SCIENCE.1231143/SUPPL_FILE/PAPV2.PDF.
46. Chen, I.; Dorr, B.M.; Liu, D.R. A General Strategy for the Evolution of Bond-Forming Enzymes Using Yeast Display. *Proc. Natl. Acad. Sci. U. S. A.* **2011**, *108*, 11399–11404, doi:10.1073/PNAS.1101046108/SUPPL_FILE/APPENDIX.PDF.